Patterned Vertical Carbon Nanotube Dry Electrodes for Impedimetric Sensing and Stimulation

Mohammad J. Abu-Saude, *Student Member, IEEE*, and Bashir I. Morshed, *Member, IEEE*

***Abstract*— Traditional wet or gel impedimetric electrodes for neuro-physiological signal (e.g., electroencephalography and electrocardiography) monitoring are usable for a short duration, as the performance of electrodes deteriorates rapidly when exposed to the environment. Dry impedimetric electrode is a promising alternative tool for long duration monitoring, however suffers from high interfacing impedance. This paper describes a novel dry interfacing electrode utilizing patterned vertical carbon nanotube (pvCNT) for impedimetric sensing. The electrodes were fabricated on circular stainless steel foil substrates (thickness = 2 mil) that are laser cut to circular discs (Ø = 10 mm). Pattern on the substrate was developed with a custom shadow mask while sputter coating the substrate with Al_2O_3 and iron. Electrically conductive multiwalled CNTs were then grown vertically in pillar formation (100 μm each side of square footprint) with various interpillar spacing (50, 100, and 200 μm for various masks). The heights of the CNT pillars were between 1 and 1.5 mm. The impedances of the electrodes were 1.92, 3.11, and 8.15 Ω for 50-, 100-, and 200-μm spacing, respectively. A comparative *in vitro* study with commercial wet and gel electrodes showed pvCNT electrode has lower interfacial impedance, comparable signal capture quality, and ability to be used for stimulation. Long duration study showed minimal impedance degradation for pvCNT electrodes over a week. The results demonstrate pvCNT is a promising dry electrode for impedimetric sensing and stimulation of neurophysiological signals over a prolonged duration.**

***Index Terms*— Dry electrode, carbon nanotubes, impedimetric interface, electrode degradation, skin–electrode interface.**

I. Introduction

ALL bioelectric neurological and physiological (neuro-physiological) signals require impedimetric interfacing with the skin for sensing of bioelectric signals or bio-impedances, such as electroencephalography (EEG), electrocardiography (ECG/EKG), electromyography (EMG), and Galvanic Skin Response (GSR) [1], [2]. These neuro-physiological signals are of clinical significance for disease diagnosis, patient monitoring, and therapy administration. Current impedimetric interfacing sensors are wet or gel based Ag/AgCl electrodes. These sensors only operates well for a short duration because of gradual degradation of conductivity, as the electrode interface impedance deteriorates over time due to evaporation, leading to signal quality degradation [3]–[6]. In addition, these wet or gel electrodes usually require skin preparation to remove dirt, skin debris, and oil from skin surface. Thus, the electrophysiology measurements suffer from two types of noises: environment and contact noise [7], [8]. The gel is a key source of the contact noise [9]. Wet or gel electrodes lead to detrimental reliability over long period; hence, the current practice is to periodically replace the electrodes, burdening the user and the operator-in-the-loop (e.g., clinician). This is a technological barrier for pervasive patient-centric care and 24/7 health/wellness monitoring at naturalistic environments that require neuro-physiological signal monitoring for prolonged periods [10]–[12].

Dry electrodes are more suitable for long duration impedimetric sensing without degrading of impedances, however suffer from inferior impedances and noise [3]–[5], [12]. Conductive polymer, such as polypyrrole (PPY) thin film on copper substrate [13] or planar plydimethylsiloxane (PDMS) [14], are promising dry electrode technologies; however, surface connectivity at the interface is poor. Improved surface connectivity and penetration through hair was achieved with PDMS based flexible pin dry electrode, which has high impedances [15]. Pin structure was also demonstrated using micro-electromechanical systems (MEMS) chips with limited pin height (250 μm) [16]. Spring-loaded mechanical metal pin electrode is another promising dry electrode with low impedance and ability to penetrate through thick layers of hair [17], [18]; however large and uncomfortable for 24/7 usage. Conductive sponge [19] and foam [3] provide comfortable interfaces, but have low electrode conductivities (e.g. more than 10 kΩ below 100 Hz). Inkjet-based dry electrode using silver ink has low electrode impedances [20], but toxicity and surface connectivity issues remain. Finally, non-contact capacitive sensors have drawn significant recent interest [21], but it mandates complex active circuitry for each sensor to deal with changing distance between sensor and scalp due to motion, high interfering noise, and issue related to sensing of potential versus charge. In general, various dry electrodes suffer from one or more unresolved issues such as low contact surface, high contact potential, polarization and high interfacial noises [8], [22]. Hence, significant research effort to search for a high performance dry electrode is still ongoing [23].

In this paper, we report a novel dry interfacing electrode based on pattered vertical carbon nanotubes (pvCNT) that

Manuscript received February 13, 2015; revised May 15, 2015; accepted June 13, 2015. Date of publication June 24, 2015; date of current version August 14, 2015. This work was supported in part by the FedEx Institute of Technology Innovation under Grant 2013-537908 and in part by the University of Memphis. The associate editor coordinating the review of this paper and approving it for publication was Dr. Chang-Soo Kim. *(Corresponding author: Bashir I. Morshed.)*

The authors are with the Department of Electrical and Computer Engineering, University of Memphis, Memphis, TN 38152 USA (e-mail: mbusaude@memphis.edu; bmorshed@memphis.edu).

Color versions of one or more of the figures in this paper are available online at http://ieeexplore.ieee.org.

Digital Object Identifier 10.1109/JSEN.2015.2449301

has very stable, low electrode impedance. The bristle-like electrode enables contact over rough skin surfaces and is breathable, thus promising high signal qualities for a prolong period of sensing. Preliminary findings were reported elsewhere [24], which is extended and elaborated here. This paper is organized as follows: Section II describes the pvCNT electrode fabrication, Section III outlines the experimental setup, Section IV details the experimental results in the same order, Section V provides some discussion items, and Section VI has concluding remarks.

II. pvCNT ELECTRODE FABRICATION

Carbon nanotube (CNT) is an extremely high aspect ratio material made of pure carbon atoms that possesses excellent electrical conductivity, thermal conductivity, mechanical strength, and chemical stability - properties that are particularly suitable to develop biosensors [25]. Multi-walled CNT (MWCNT) and some configurations of single-wall CNT (SWCNT), such as armchair configuration, show metal-like electric-conductivity properties [26]. In vitro studies have demonstrated that CNT based biosensors can provide reliable interfacing to neuronal signals [25]. Furthermore, at a low concentration external to the body, CNT based biosensors do not show toxicity [27]–[29]. Even though attempts were made to develop neurological and physiological electrodes with CNT, previous attempts for direct use of CNT as dry electrode interfaces had only limited success [9], [30]–[32]. We note two prime limitations that might have hampered the potential of CNT electrodes: (1) CNTs were uniformly grown on the substrate without any gap, which led to a dense surface of CNT tips at the top of the electrode, unable to make good contact through skin roughness and pores, and (2) the height of the grown CNTs were small, in the range of tens of μm, which would not cause any significant penetration through the skin ridges. Other techniques that utilized CNT as dry electrodes primarily involve integration of CNT within other polymers or substrates (such as PPY, and PDMS) [33]–[35] that do not have good electrical conductivity, and suffer from the issues like the top surface of the composite electrode is planar, thus would not make proper contact through the rough skin surface.

The prototyped pvCNT electrode is different than previously developed CNT electrodes in the aspect that the CNTs are grown in custom patterns resulting in bristle-like structure. Furthermore, the growth of CNT is vertically aligned and can be long (e.g., 1.5 mm); that is sufficient to penetrate through pores and ridges of the skin. The electrode fabrication was performed through a commercial CNT fabrication facility (NanoLab, Boston, MA). Briefly, the procedure was as follows. Typical catalyst deposition processing for aligned nanotube growth was used, which includes the deposition of 10 nm of Al_2O_3, followed by 1-2 nm of iron, both by sputtering processes. For a patterned array, the photoresist is imaged and developed, and both alumina and iron are subsequently deposited through the holes in the mask. After sputtering, the resist is stripped, and the patterned substrates are subjected to thermal growth of carbon nanotubes. Aligned nanotube growth is typically accomplished in several steps: heat-up, anneal, growth, and cool-down. During the heat-up

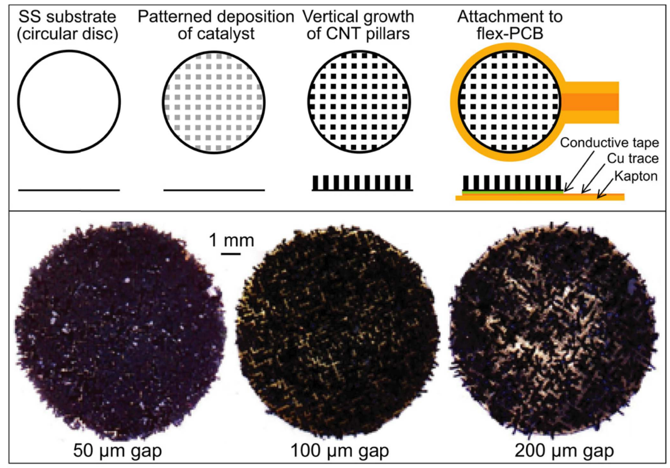

Fig. 1. (Top) Schematic diagram of the pvCNT electrode fabrication process. (Bottom) Photographs of three pvCNT electrodes with various pillar separations (50, 100, and 200 μm).

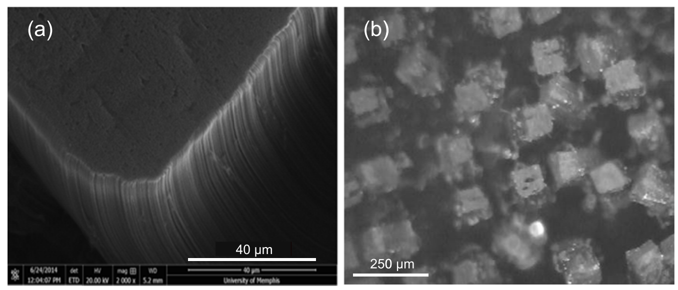

Fig. 2. (a) A SEM image of a pvCNT pillar top corner depicting individual CNT strands aligned vertically. (b) An optical microscope image showing the bristle-like arrangement of the pillars (100 μm spacing).

and annealing stage, the catalyst film breaks into islands, which will determine the diameter and site density of the carbon nanotubes that will be nucleated. The substrates are loaded into a 500°C furnace for rapid annealing, and then removed until the system is at the growth temperature, where the substrate is reinserted for CNT growth.

For this study, we have fabricated pvCNT electrodes using MWCNT primarily due to its superior electrical (conductivity) and mechanical (elasticity and tensile strength) properties [9]. The fabricated pvCNT electrode is an ensemble of an array of MWCNT in pillar formation of 100 μm-squared footprints. The square grid formation array of pillars was grown on a circular stainless steel (SS) foil substrate (Ø = 10 mm, 2 mils thick). The pvCNT pillars had heights of 1 to 1.5 mm and were grown vertically. Here, we report results from three spacing between the pillars: 50, 100 and 200 μm. These initial prototypes were fabricated in simple square geometric patterns for proof-of-concept, but fabrication of other geometric patterns is trivial. Fabrication process and pvCNT samples with different spacing are depicted in Fig. 1.

Optical microscopy and Scanning Electron Microscopy (SEM) images revealed the top of the electrodes have bristle-like arrangements. SEM images were captured at the Integrated Microscopy Center (IMC) of the University of Memphis. In Fig. 2, a SEM image shows the corner of

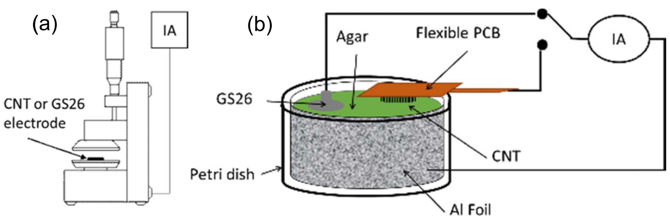

Fig. 3. Impedance measurement setups: (a) Fixture 16451B setup for sensor impedance measurement. (b) Interfacial impedance measurement with agar gel setup. (IA: Impedance Analyzer).

a pvCNT pillar depicting aligned individual CNT fibers, while an optical microscope image shows the top of the pillar arrangement of a 100 μm spaced pvCNT electrode. Note that even though the pvCNT pillars were patterned in square array formations at the substrate, the top of the pvCNT pillars appear in non-uniform formation due to natural bending of the pvCNT pillars (height vs width aspect ratio is greater than 10:1), as evident in the SEM and optical images of Fig. 2.

III. Experimental Setup and Procedure

A. Impedance Measurements

The impedance of the prototyped pvCNT electrodes of various spacing and that of some commercial electrodes (GS-26, Bio-Medical Instruments, USA, and Emotiv, San Francisco, CA) were analyzed by Agilent 4294A Precision Impedance Analyzer (Agilent Technologies Inc., Santa Clara, CA, USA) using two fixtures (16451B and 16089B) at room temperature (~23°C). Prior to each measurement, all fixtures were compensated and calibrated as per manufacturer instruction to ensure accurate measurements. Two software tools, MATLAB (MathWorks, Natick, MA, USA) and Microsoft Excel (Microsoft Corp, Redmond, WA, USA) were utilized to periodically collect data via a GPIB to USB cable, and to analyze the collected data from the impedance analyzer.

1) Sensor Impedance Measurement Using a Dielectric Fixture: Agilent 4294A Impedance Analyzer (IA) with a Dielectric Fixture 16451B was used to measure the impedance of the pvCNT and GS-26 electrodes. The electrodes were positioned between the parallel plates of the fixture. During the pvCNT measurement, it was ensured that the two plates barely contacted the bottom surface, i.e. SS substrate of the pvCNT electrode (Fig. 3a). Measurement of the impedance of pvCNT electrodes was collected using Fixture 16451B with barely touching CNT tips (at single click of the torque knob). The same procedure was applied for the GS-26 electrode measurement. The frequency range of the impedance analyzer was set to scan from 40 Hz to 100 kHz.

2) Interfacial Impedance Measurement With Agar Gel: For interfacial impedance measurements, a skin phantom model was built with agar gel. Briefly, the preparation of agar was as follows. First, 4.35 gm of sodium chloride (NaCl) and 15 gm of agar powder (A10752, Alfa Aesar) were added to 500 mL of water. The solution was then boiled at 75°C for a few hours, then poured into an Al foil wrapped petri dish, and naturally cooled. A flexible PCB (flex-PCB) was designed and prototyped (Cirexx Intl., CA, USA), which allowed pvCNT sensor to be attached at one end and provides low impedance electrical connectivity at the other end. A pvCNT electrode was affixed on the exposed Cu pad (Ø = 10 mm) of the flex-PCB via a double-sided z-axis conductive tape (Electrically Conductive Adhesive Transfer Tape 9703, 3M Company, MN, USA). The electrode was placed (pvCNT facing down) on top of agar and connected to the impedance analyzer via Agilent Fixture 16089B, while the other terminal of the fixture was connected to the Al foil (Fig. 3b).

B. Long Duration Study

One of the significant benefits of dry electrodes is their stable operation over a long duration. For this stability test, we tested impedances of commercial gel and wet electrodes (GS-26 and Emotiv, respectively) in contrast to pvCNT dry electrodes. As electrolyte is used in wet or gel electrodes to reduce skin-electrode interfacial impedance, based on chemical compositions, these interfaces become dry within hours due to evaporation of the electrolyte leading to significant increases or fluctuations of the impedances. In these long duration studies, the pvCNT, GS-26, and Emotiv electrode impedances were monitored over for 24 hours and for 7 days. Fixture 16451B was used in this study and the data acquisition software was programmed to automatically collect impedance data every 1 hour (for 24-hour study) or every 4 hours (for 7-day study).

C. Signal Capture in Bench Test

When the electrodes capture neuro-physiological signals from human body, there are number of factors that affect the measurements. For instance, half-cell potential is usually observed for wet or gel electrode, which arises from the potential differences across the interface between anions and cations. This shows up as a DC offset in ECG, EMG and other bioelectric signal capture electrodes. For dry electrodes, motion artifact and micro-movement are sources of noise in these measurements, which stems from relative movements of the electrodes with respect to the skin surface (micro-movement) producing fluctuations in measurements. We have used agar gel as skin phantom model in a bench-top setup to study quality of the captured signals. The signal was applied to an Al foil at the bottom, while measurements were taken with the sensors (GS-26 and pvCNT electrodes) at the top of the agar.

D. Stimulation Study Using pvCNT

For stimulation experiments with the electrodes, the same procedure as mentioned in the signal capture section was used, except the signal was applied to the top surface of the agar gel using the pvCNT electrode (stimulated signal), while the signal was recorded from the Al foil (measured signal).

E. Compression and Peel Tests

Mechanical compression was applied with the test fixture 16451B, where a small pressure can be applied

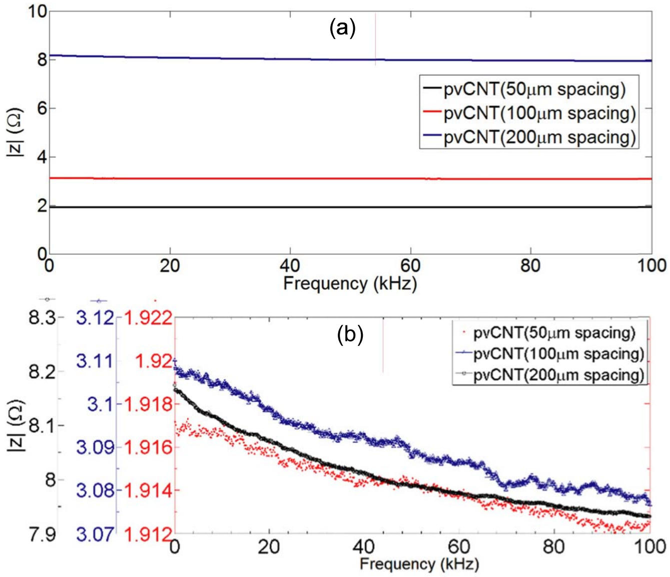

Fig. 4. (a) The amplitude of the impedance of pvCNT electrode with three pillar spacings (50, 100, and 200 μm). (b) The amplitude variations of the impedances are magnified using three separate y-axis markers, which show slight decrease of impedance with higher frequencies.

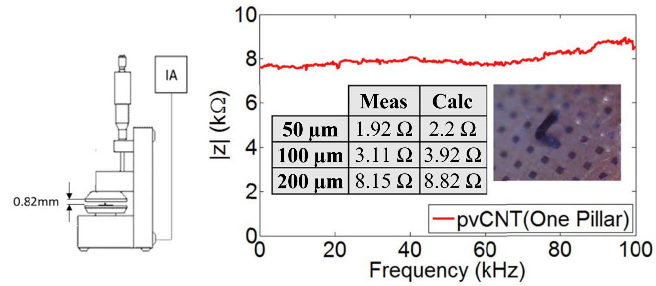

Fig. 5. The amplitude of the impedance of single pillar of pvCNT electrode. The table inset shows measured (Meas) and calculated (Calc) resistances for various spacing of pvCNT electrodes.

by twisting the torque screw. Scanning electron microscopy (SEM) pictures were taken before and after the experiments. To measure tensile strength of the pvCNT with the substrate, peel tests were conducted by holding the bottom of the sensor to a double sided tape, while a drafting tape was attached to the top surface of the carbon nanotubes and then peeled off at a $\sim 45°$ angle. A mini-digital microscope camera (Vividia 2.0MP Handheld USB Digital Microscope, Oasis Scientific Inc., Taylors, SC, USA) was used to inspect the samples after each peel test.

IV. Experimental Results

The experimental results are described in this section in the same order of experimental setup described in the last section.

A. Impedance Measurement

1) Sensor Impedance Measurement Using a Dielectric Fixture: The results here are presented in terms of the amplitude (|Z|) and the phase angle (θ) of the impedance. Fig. 4 shows the plot of the absolute impedance (|Z|) for electrodes with 50, 100, and 200 μm gaps between pvCNT pillars. At 40 Hz, the impedance of 50, 100, and 200 μm spacing electrodes were 1.92, 3.11, and 8.15 Ω, respectively. Higher variation of impedance with frequency was observed for larger spacing. For instance, the variation of impedance for 50 μm spacing of electrodes from 40 Hz to 100 kHz is 6 mΩ, whereas for 200 μm spacing, the variation is 243 mΩ. A lower spacing between pillars leads to a higher number of pillars per unit area; therefore, the corresponding impedance is lower. As expected, the pvCNT electrode with the least spacing (50 μm) showed the least impedance (as a higher number of pillars per unit area are conducting in parallel), compared to other samples (where lesser numbers of pillars are conducting per unit area).

To measure the impedance of a single pillar (100 μm $\times$ 100 μm base area), we have manually plucked all the pillars of an electrode using tweezers except one pillar at the center of the substrate. The resistance of the single pillar is measured to be 7.6 kΩ at 40 Hz. Using this information, resistances for various gaps can be calculated and correlated with the corresponding measured values. For instance, the number of the pillars for 200 μm spacing can be calculated to be 873 pillars using a geometric approximation approach. Hence, the calculated total resistance is 8.82 Ω, as pvCNT pillars are in parallel formation. The computed result closely matches with the experimental measurement of 8.15 Ω (Fig. 4). The impedance of a single pvCNT pillar on a SS substrate and a table shows the measured and calculated values of pvCNT electrode resistances for various inter-pillar gaps are shown in Fig. 5.

2) Interfacial Impedance Measurement With Agar Gel: As described in the method section, two electrodes were tested in these experiments: a commercial gel type ECG electrode (GS-26), and a pvCNT dry electrode. The pvCNT electrode was mounted on a flex-PCB using z-axis conductive tape as mentioned in the previous section. Fig. 6(a-c) presents the photographs of the mounted pvCNT electrode. Fig. 6(d-e) shows plots of interfacial impedances (amplitude and phase) of both electrodes with agar gel model of skin (Fig. 3b). This interfacial impedance includes a series combination of the impedance of the electrode, the impedance of the agar, the impedance of the Al foil, the electrode-agar contact impedance, and the Al foil-agar contact impedance. The impedance of the pvCNT in range up to 300 Hz is significantly lower than the impedance of the gel electrode, while the phase distortion is superior up to kHz range. Furthermore, the worst-case impedance and phase distortion is equivalent to commercial gel electrode. As the electrode impedance itself is very small (Fig. 4), it is plausible that at higher frequencies, the agar impedance dominates over the electrode impedance as the electrode-agar interfacial reactance decreases, thus both electrode characteristics show similar performances.

B. Long Duration Study

In the first experiment of long duration study, the impedance measurements were captured for over 24 hours for pvCNT and GS-26 gel electrodes. The impedance data was recorded

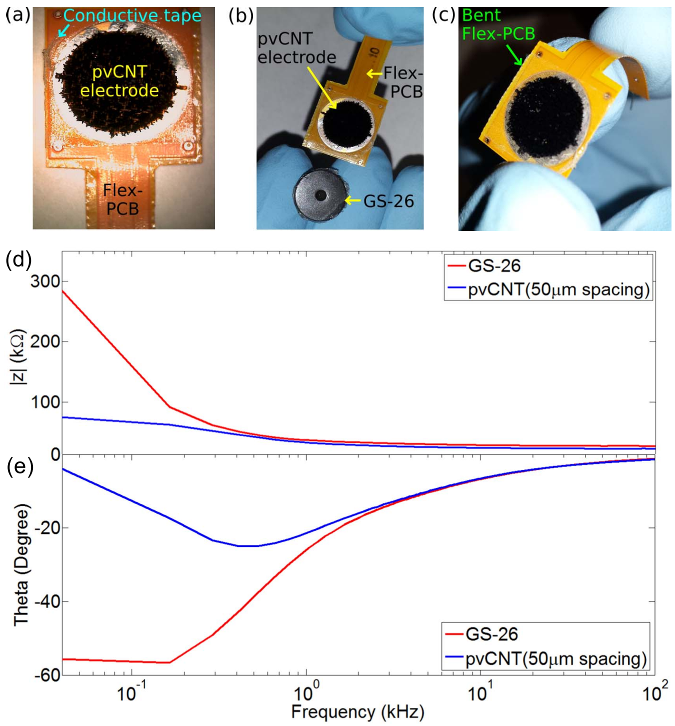

Fig. 6. (a-c) Photographs of pvCNT electrode on flex-PCB. (d-e) The interfacial impedance (magnitude and phase) with agar gel using two electrodes: gel electrode (GS-26) and prototyped pvCNT electrode.

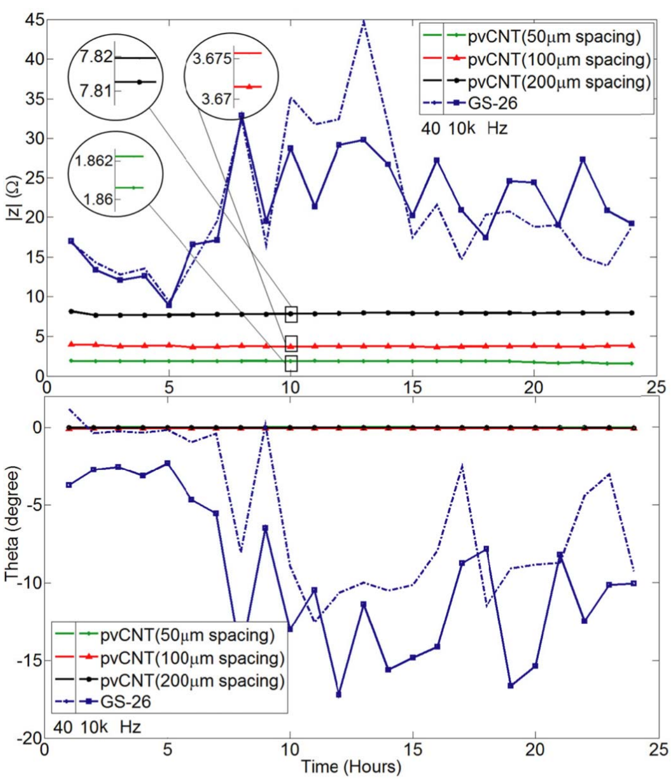

Fig. 7. The amplitude and the phase results from impedance measurement of four electrodes over 24 hours.

for the frequency ranges of 40 Hz to 100 kHz. Fig. 7 shows the measurements of these electrodes for two frequencies (40 Hz and 10 kHz) for 24 hours. In case of pvCNT electrodes,

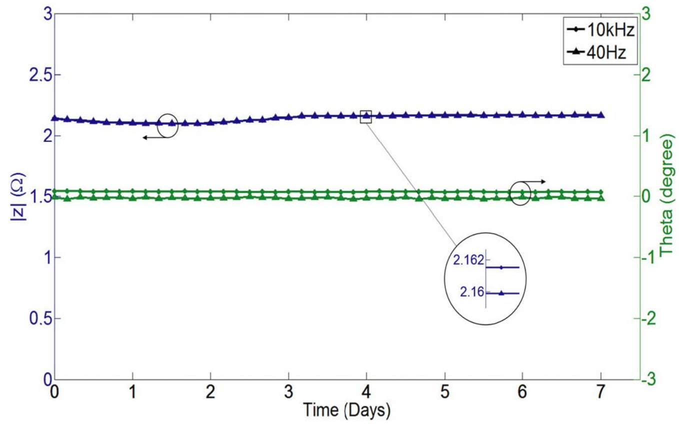

Fig. 8. A long-term study result of the impedance of pvCNT dry electrodes (50 μm spacing) over 7 days.

the amplitude and the phase of the impedance values change very slightly over the duration (within 1 Ω and 1° variations over 24 hours). In case of GS-26 gel electrode, the impedance changes more significantly, especially after 8 hours, the average amplitude and phase of the impedance variation was over 10 Ω and 10°, respectively. The frequency response of GS-26 (compared between 40 Hz and 10 kHz) also changes widely, while pvCNT electrodes show very stable behavior on both frequencies. The frequency dependent impedance difference for 40 Hz and 10 kHz are is about 5 mΩ as shown in the insets of the Fig. 7(a).

The pvCNT electrode was also tested for weeklong experiments to show that the degradation of the impedance is minimal. The software was programed to collect the data every 4 hours over 11.5 days. Fig. 8 shows a representative impedance (magnitude and phase) changes over 7 days using an electrode with 50 μm spacing.

Another experiment compared a commercial Emotiv wet electrode (Emotiv, San Francisco, CA) in contrast to pvCNT electrodes. Fig. 9 shows the results of this experiment over 24-hour duration. As the Emotiv electrode is wet type, it becomes dry within a few hours. Thus, the amplitude and the phase of the impedance change significantly, and signal capture becomes unreliable. After 24 hours, the amplitude of the impedance of wet electrode has increased by about two orders of magnitude (Fig. 9), while the pvCNT dry electrode impedance remained very stable for the same period.

C. Signal Capture in Bench Test

It is important to determine the half-cell potential for pvCNT electrode. Experimental results showed that the potential drops of the electrodes interfaced with Al foil are 809.4 mV and 15 mV for GS-26 electrode and pvCNT electrode, respectively. A snapshot of captured signal is shown in Fig. 10(a) where the applied signal was a sinusoidal of 100 Hz. Fig. 10(b) shows the snapshot of a signal captured in bench test with agar using a simulated ECG signal from a function generator applied to the Al foil at the bottom surface of the agar (setup as shown in Fig. 3). Data captured from the electrodes (GS-26 and pvCNT) shows comparable signal capture capabilities of both electrodes.

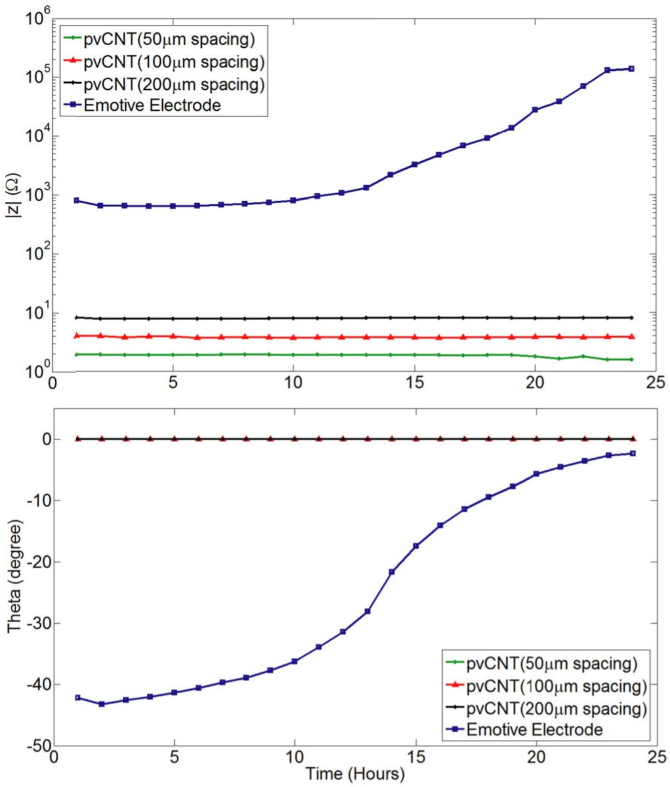

Fig. 9. The impedance of a wet electrode in comparison to the prototyped pvCNT dry electrodes (50, 100 and 200 μm spacing) over 24 hours.

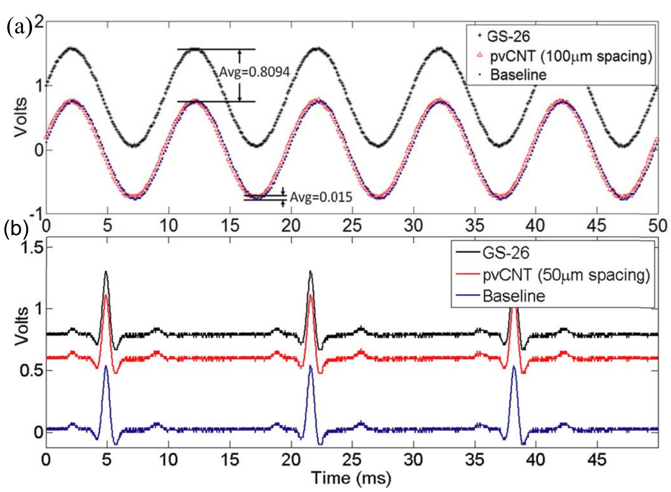

Fig. 10. (a) Signal capture by pvCNT electrode and GS-26 electrode interfaced with an Al foil. (b) Signal capture by pvCNT electrode and GS-26 electrode interfaced with an agar gel phantom model.

D. Stimulation Study Using pvCNT

A pulse signal is applied to the top of the agar every one-second with 200 ms of duty cycle and pvCNT is used as stimulations electrode for this experiment. The signals were measured from the other side of the agar gel (Al foil). Fig. 11(a) shows that the phase shift between the stimulated and the measured signal is 0.8 ms, whereas the potential drops on the electrode and agar interface are −592 mV. There was no extra weight or force applied during the experiment and there was insignificant change of the pvCNT pillars from the stimulation experiments, as shown in Fig. 11(b).

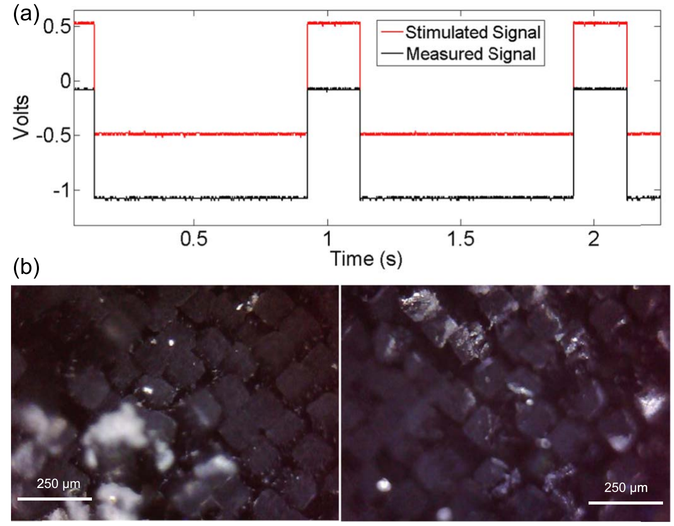

Fig. 11. (a) Signal stimulated by pvCNT electrode and measured from the AL foil. (b) Optical microscopy images of a pvCNT pillars (50 μm spacing) prior (left) and after (right) the experiment.

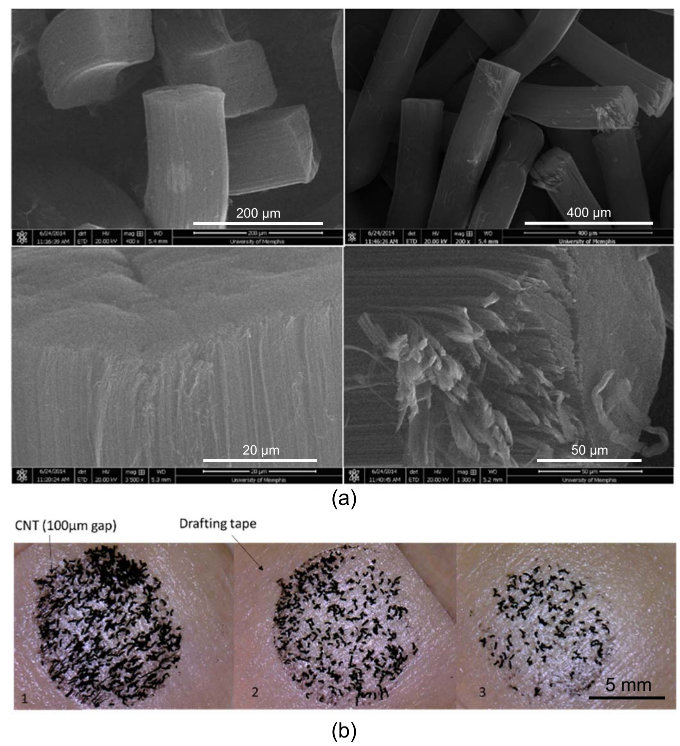

Fig. 12. (a) SEM images of pvCNT electrodes after the compression experiments. Top: Bending of pvCNT pillar (Left: 100 μm spacing, Right: 200 μm spacing). Bottom: Breakdown of pvCNT pillar after the compression experiments (Left: Slight peeling effect, Right: Complete breakdown). (b) A representative result of peel tests showing peeled pillars on the drafting tape in 3 successive attempts (labeled as 1-3) with a pvCNT electrode (100 μm spacing).

E. Compression and Peel Tests

We have conducted compression and peel tests to test mechanical stability. Some representative results are depicted in Fig. 12. In Fig. 12(a), SEM images of the pvCNT electrode are shown after the compression test experiments. It is observed that the pvCNT pillars bend with compression force. High compression force can even cause disintegration of pvCNT pillar formation as evident from Fig. 12(a). The peel test demonstrated that pvCNT pillars could be dislodged with the drafting tape test as depicted in Fig. 12(b), showing three successive peel test on a pvCNT electrode.

V. Discussions

The impedances of dry polymer foam [2] and printed [20] electrodes were reported to be almost similar of commercial wet electrodes, and that of PDMS based dry sensor [14] was about one order smaller. In comparison, the pvCNT electrode impedances were measured to be two orders smaller than that of the wet electrodes. The foam electrode was reported to be stable for 5 hours [2], whereas this long duration study showed that pvCNT electrodes had stable impedances for one week.

Furthermore, in contrast to the other dry electrodes, due to the structure of pvCNT pillars with spacing that allows airflow, pvCNT electrode has better breathability. The bristle-like arrangement of the pvCNT electrode will also promote good contact over rough skin surfaces and pores. As small concentration of carbon nanotubes are shown to be not toxic on the epidermal tissue and due to low possibility of skin puncture, the pvCNT electrode can possibly be safer to use.

VI. Conclusion

A novel dry pvCNT electrode is demonstrated in this paper for physiological and neurological bioelectric or impedimetric signal capture. The electrodes were fabricated by patterning vertically aligned CNT pillars on a circular disk (Ø = 10 mm) of SS foil. The characteristics of pvCNT were assessed against a commercial gel electrode (GS-26) and a wet electrode (Emotiv). The pvCNT has shown stable impedance over short and long durations. The impedances of pvCNT electrodes were found to be a function of the pillar spacing. The pvCNT electrodes also showed a lower electrical impedance and comparable signal capture in bench test with simulated signals. Results show that pvCNT dry electrode can be a very suitable for long duration neuro-physiological signal collection. The pvCNT electrode was also tested for stimulation. This study demonstrates the pvCNT electrode as a promising technology for dry electrode for impedimetric sensing and stimulation over long durations.

Acknowledgement

The authors would like to thank Sergi Consul-Pacareu for his valuable contribution enabling this work. They would also like to thank the anonymous reviewers and editors for their valuable comments, suggestions, and insights to improve the quality of this manuscript.

References

[1] S. Grimnes and O. G. Martinsen, *Bioimpedance and Bioelectricity Basics*. Bodmin, U.K.: Academic, 2000.

[2] R. Plonsey and R. C. Barr, *Bioelectricity: A Quantitative Approach*, 3rd ed. New York, NY, USA: Springer, 2007.

[3] C. Lin, L. Liao, Y. Liu, I. Wang, B. Lin, and J. Chang, "Novel dry polymer foam electrodes for long-term EEG measurement," *IEEE Trans. Biomed. Eng.*, vol. 58, no. 5, pp. 1200–1207, May 2011.

[4] A. Searle and L. Kirkup, "A direct comparison of wet, dry and insulating bioelectric recording electrodes," *Physiol. Meas.*, vol. 21, no. 2, pp. 271–283, May 2000.

[5] Y. M. Chi, T.-P. Jung, and G. Cauwenberghs, "Dry-contact and noncontact biopotential electrodes: Methodological review," *IEEE Rev. Biomed. Eng.*, vol. 3, pp. 106–119, Oct. 2010.

[6] C. Guger, G. Krausz, B. Z. Allison, and G. Edlinger, "Comparison of dry and gel based electrodes for P300 brain–computer interfaces," *Front Neurosci.*, vol. 6, no. 60, pp. 1–7, May 2012, doi: 10.3389/fnins.2012.00060.

[7] E. Huigen, A. Peper, and C. A. Grimbergen, "Investigation into the origin of the noise of surface electrodes," *Med. Biol. Eng. Comput.*, vol. 40, no. 3, pp. 332–338, May 2002.

[8] J. G. Webster, *Medical Instrumentation: Application & Design*. New York, NY, USA: Wiley, 1998.

[9] G. Ruffini *et al.*, "A dry electrophysiology electrode using CNT arrays," *Sens. Actuators A, Phys.*, vol. 132, no. 1, pp. 34–41, Apr. 2006.

[10] S. Patel, H. Park, P. Bonato, L. Chan, and M. Rodgers, "A review of wearable sensors and systems with application in rehabilitation," *J. NeuroEng. Rehabil.*, vol. 9, p. 21, Apr. 2012.

[11] H. Alemdar and C. Ersoy, "Wireless sensor networks for healthcare: A survey," *Comput. Netw.*, vol. 54, no. 15, pp. 2688–2710, Oct. 2010.

[12] B. He *et al.*, "Grand challenges in mapping the human brain: NSF workshop report," *IEEE Trans. Biomed. Eng.*, vol. 60, no. 11, pp. 2983–2992, Nov. 2013.

[13] S. Jamadade, S. Jadhav, and V. Puri, "Electromagnetic properties of polypyrrole thin film on copper substrate," *Arch. Phys. Res.*, vol. 1, no. 4, p. 205, 2010.

[14] J.-Y. Baek, J. An, J. Choi, K. Park, and S. Lee, "Flexible polymeric dry electrodes for the long-term monitoring of ECG," *Sens. Actuators A, Phys.*, vol. 143, no. 2, pp. 423–429, 2008.

[15] L.-F. Wang, J.-Q. Liu, B. Yang, and C.-S. Yang, "PDMS-based low cost flexible dry electrode for long-term EEG measurement," *IEEE Sensors J.*, vol. 12, no. 9, pp. 2898–2904, Sep. 2012.

[16] J.-C. Chiou *et al.*, "Using novel MEMS EEG sensors in detecting drowsiness application," in *Proc. IEEE Biomed. Circuits Syst. Conf.*, London, U.K., Nov./Dec. 2006, pp. 33–36.

[17] R. Matthews *et al.*, "Real time workload classification from an ambulatory wireless EEG system using hybrid EEG electrodes," in *Proc. 30th Annu. Int. Conf. IEEE Eng. Med. Biol. Soc.*, Aug. 2008, pp. 5871–5875.

[18] C. Grozea, C. D. Voinescu, and S. Fazli, "Bristle-sensors—Low-cost flexible passive dry EEG electrodes for neurofeedback and BCI applications," *J. Neural Eng.*, vol. 8, no. 2, pp. 025008-1–025008-14, Apr. 2011.

[19] A. Gruetzmann, S. Hansen, and J. Müller, "Novel dry electrodes for ECG monitoring," *Phys. Meas.*, vol. 28, no. 11, pp. 1375–1390, Oct. 2007.

[20] L. Xie, Y. Geng, M. Mantysalo, L.-L. Xu, F. Jonsson, and L.-R. Zheng, "Heterogeneous integration of bio-sensing system-on-chip and printed electronics," *IEEE J. Emerg. Sel. Topics Syst.*, vol. 2, no. 4, pp. 672–682, Dec. 2012.

[21] T. J. Sullivan, S. R. Deiss, G. Cauwenberghs, and T. Jung, "A low-noise low-power EEG acquisition node for scalable brain-machine interfaces," *Proc. SPIE Conf. Bioengineered Bioinspired Syst. III*, vol. 6592, pp. 659203-1-8, May 2007.

[22] C. Gondran, E. Siebert, P. Fabry, E. Novakov, and P. Y. Gumery, "Non-polarisable dry electrode based on NASICON ceramic," *Med. Biol. Eng. Comput.*, vol. 33, no. 3, pp. 452–457, May 1995.

[23] S. Ha *et al.*, "Integrated circuits and electrode interfaces for noninvasive physiological monitoring," *IEEE Trans. Biomed. Eng.*, vol. 61, no. 5, pp. 1522–1537, May 2014.

[24] M. Abu-Saude, S. Consul-Pacareu, and B. I. Morshed, "Feasibility of patterned vertical CNT for dry electrode sensing of physiological parameters," in *Proc. IEEE Topical Conf. Biomed. Wireless Technol., Netw., Sensing Syst. (BioWireleSS)*, Jan. 25–28, 2015, pp. 1–4.

[25] Y. Zhang, Y. Bai, and B. Yan, "Functionalized carbon nanotubes for potential medicinal applications," *Drug Discovery Today*, vol. 15, nos. 11–12, pp. 428–435, Jun. 2010.

[26] C. T. White and T. N. Todorov, "Carbon nanotubes as long ballistic conductors," *Nature*, vol. 393, pp. 240–243, May 1998.

[27] L. Bareket-Keren and Y. Hanein, "Carbon nanotube-based multi electrode arrays for neuronal interfacing: Progress and prospects," *Frontiers Neural Circuits*, vol. 6, Jan. 2013, Art. ID 122, doi: 10.3389/fncir.2012.00122.

[28] S. K. Smart, A. I. Cassady, G. Q. Lu, and D. J. Martin, "The biocompatibility of carbon nanotubes," *Carbon*, vol. 44, no. 6, pp. 1034–1047, May 2006.

[29] J. Chłopek, B. Czajkowska, B. Szaraniec, E. Frackowiak, K. Szostak, and F. Béguind, "In vitro studies of carbon nanotubes biocompatibility," *Carbon*, vol. 44, no. 6, pp. 1106–1111, May 2006.

[30] G. Ruffini *et al.*, "ENOBIO—First tests of a dry electrophysiology electrode using carbon nanotubes," in *Proc. 28th Annu. Int. Conf. IEEE EMBS*, New York, NY, USA, 2006, pp. 1826–1829.

[31] G. Ruffini *et al.*, "First human trials of a dry electrophysiology sensor using a carbon nanotube array interface," *Sens. Actuators A, Phys.*, vol. 144, no. 2, pp. 275–279, Jun. 2008.

[32] J. K. Radhakrishnan *et al.*, "Growth of CNT array for physiological monitoring applications," *Proc. SPIE Conf. Nanosens. Microsens. Bio-Syst.*, vol. 6931, pp. 69310P-1-5, Mar. 2008.

[33] H. B. Baskey, "Development of carbon nanotube based sensor for wireless monitoring of electroencephalogram," *DRDO Sci. Spectr.*, vol. 59, no. 1, pp. 161–163, Mar. 2009.

[34] H.-C. Jung *et al.*, "CNT/PDMS composite flexible dry electrodesfor long-term ECG monitoring," *IEEE Trans. Biomed. Eng.*, vol. 59, no. 5, pp. 1472–1479, May 2012.

[35] P. Rai, J. Lee, G. N. Mathur, and V. K. Varadan, "Carbon nanotubes polymer nanoparticles inks for healthcare textile," *Proc. SPIE Nanosyst. Eng. Med.*, vol. 8548, p. 854822, Oct. 2012, doi: 10.1117/12.946253.

Mohammad J. Abu-Saude (S'14) received the B.Sc. degree in computer engineering from Yarmouk University, Irbid, Jordan, in 2003, and the M.Sc. degree in electrical and computer engineering from the University of Memphis, Memphis, TN, USA, in 2013. He is currently pursuing the Ph.D. degree in electrical and computer engineering with the University of Memphis.

He was a Research Assistant with the ESARP Laboratory, University of Memphis, from 2011 to 2015. His research interests include nanotechnology based dry electrode, passive body-worn sensors, and embedded cyber-physical systems.

Bashir I. Morshed (M'12) received the B.Sc. degree in electrical and electronics engineering from the Bangladesh University of Engineering and Technology, Dhaka, Bangladesh, in 2001, the M.Sc. degree in electrical and computer engineering from the University of Windsor, ON, Canada, in 2004, and the Ph.D. degree in electrical and computer engineering from the Electronics Department, Carleton University, ON, Canada, in 2010.

Since 2011, he has been an Assistant Professor with the Electrical and Computer Engineering Department, University of Memphis, Memphis, TN, USA. His research interests include embedded systems, cyber physical systems, fully-passive sensors, dry impedimetric sensors, neuro-physiological signal processing, and implantable drug delivery systems. He received the prestigious Canadian Commonwealth Fellowship in 2002.